Quarkonia and Heavy Flavor at LHCb and PHENIX

Krista Smith

INT-22-3: Heavy Flavor Production in Heavy-Ion and Elementary Collisions

October 13, 2022

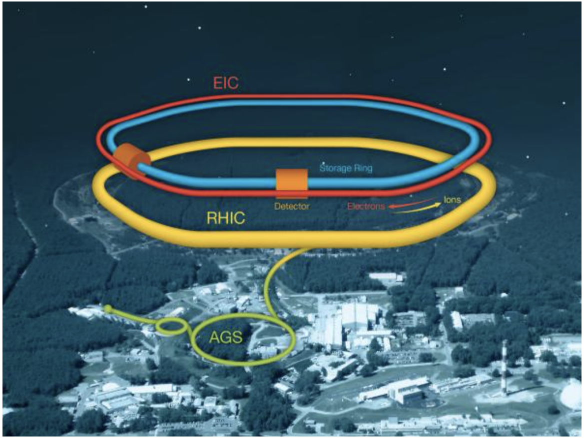

Brief Introduction

LHCb Experiment

- The **primary purpose of the LHCb experiment** is to try and understand why the universe appears to be composed almost entirely of matter, but no antimatter
- LHCb recording data 2010-present
- 634 physics papers published
- Not specifically designed for heavy-ion collisions
- Top 4 most cited papers with 4,907 citations

Observation of $J/\psi p$ Resonances Consistent with Pentaquark States in $\Lambda_b^0 \to J/\psi K^- p$ Decays #2
LHCb Collaboration • Roel Aaij (CERN) et al. (Jul 13, 2015)
Published in: *Phys.Rev.Lett.* 115 (2015) 072001 • e-Print: 1507.03414 [hep-ex]
pdf links DOI cite claim 1,456 citations

Test of lepton universality using $B^+ \to K^+\ell^+\ell^-$ decays #3
LHCb Collaboration • Roel Aaij (NIKHEF, Amsterdam) et al. (Jun 25, 2014)
Published in: *Phys.Rev.Lett.* 113 (2014) 151601 • e-Print: 1406.6482 [hep-ex]
pdf DOI cite claim 1,244 citations

Test of lepton universality with $B^0 \to K^{*0}\ell^+\ell^-$ decays #4
LHCb Collaboration • R. Aaij (CERN) et al. (May 16, 2017)
Published in: *JHEP* 08 (2017) 055 • e-Print: 1705.05802 [hep-ex]
pdf links DOI cite datasets claim 1,132 citations

Measurement of the ratio of branching fractions $\mathcal{B}(\bar{B}^0 \to D^{*+}\tau^-\bar{\nu}_\tau)/\mathcal{B}(\bar{B}^0 \to D^{*+}\mu^-\bar{\nu}_\mu)$ #5
LHCb Collaboration • Roel Aaij (CERN) et al. (Jun 29, 2015)
Published in: *Phys.Rev.Lett.* 115 (2015) 11, 111803, *Phys.Rev.Lett.* 115 (2015) 15, 159901 (erratum) • e-Print: 1506.08614 [hep-ex]
pdf links DOI cite claim 1,075 citations

Inspire HEP citation list (as of October 10, 2022)

LHCb Detector Upgrade

⋆ See Matt Durham's talk, Week 3

Runs 1 & 2

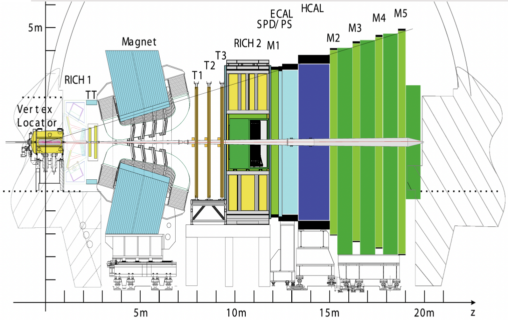

Runs 3–4

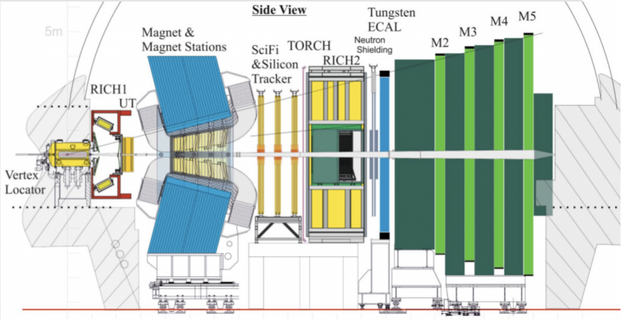

- Designed for searches of new physics in beauty and charm hadron decays ⋆
  - Measures particles from $p_T > 0$ at forward pseudorapidity $2 < \eta < 5$
- LHCb tracking fully upgraded for Run 3 (2022–2026)

PHENIX Experiment

- The **primary purpose of the PHENIX experiment** was to detect and characterize the Quark Gluon Plasma (QGP) using data collected from A + A, p + A, and pp collisions
- PHENIX recorded data 1999-2016
- 210 physics papers published
- Specifically designed for heavy-ion collisions
- Top 4 most cited papers with 6,281 citations

Formation of dense partonic matter in relativistic nucleus-nucleus collisions at RHIC: Experimental evaluation by the PHENIX collaboration #1
PHENIX Collaboration • K. Adcox (Vanderbilt U.) et al. (Oct, 2004)
Published in: *Nucl.Phys.A* 757 (2005) 184-283 • e-Print: nucl-ex/0410003 [nucl-ex]
pdf DOI cite claim 3,302 citations

Suppression of hadrons with large transverse momentum in central Au+Au collisions at $\sqrt{s_{NN}}$ = 130-GeV #2
PHENIX Collaboration • K. Adcox (Vanderbilt U.) et al. (Sep, 2001)
Published in: *Phys.Rev.Lett.* 88 (2002) 022301 • e-Print: nucl-ex/0109003 [nucl-ex]
pdf DOI cite datasets claim 1,156 citations

Identified charged particle spectra and yields in Au+Au collisions at S(NN)1/2 = 200-GeV** #3
PHENIX Collaboration • S.S. Adler (Brookhaven) et al. (Jul, 2003)
Published in: *Phys.Rev.C* 69 (2004) 034909 • e-Print: nucl-ex/0307022 [nucl-ex]
pdf DOI cite datasets claim 977 citations

Elliptic flow of identified hadrons in Au+Au collisions at s(NN)(1/2) = 200-GeV** #4
PHENIX Collaboration • S.S. Adler (Brookhaven) et al. (May, 2003)
Published in: *Phys.Rev.Lett.* 91 (2003) 182301 • e-Print: nucl-ex/0305013 [nucl-ex]
pdf DOI cite claim 846 citations

Inspire HEP citation list (as of October 10, 2022)

PHENIX Muon and Central Arms

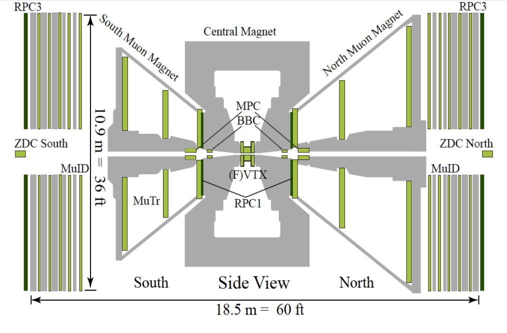

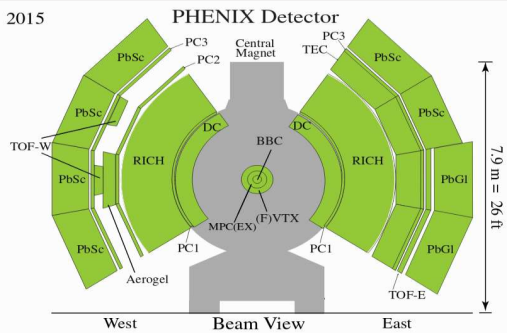

- Muon arms measure muons and unidentified charged hadrons
- Mid-rapidity arms measure electrons, photons and identified hadrons
- The PHENIX detector has been fully dissembled and replaced by sPHENIX

Recent LHCb and PHENIX analyses focus on the following collision systems and present the following measurements:

- pp collisions at $\sqrt{s} = 5$, 8, and 13 TeV
- p**Pb** collisions at $\sqrt{s_{NN}} = 8.16$ TeV
- **PbPb** collisions at $\sqrt{s_{NN}} = 5$ TeV
- pp, p**Al**, p**Au**, **Cu+Au**, **Au+Au** collisions at $\sqrt{s_{NN}} = 200$ GeV

1. J/ψ production and polarization
2. J/ψ elliptic flow
3. Fixed target J/ψ and D^0 production
4. J/ψ and $\psi(2S)$ production in UPC
5. Bottomonium nuclear modification
6. $b\bar{b}$ production
7. ϕ-meson nuclear modification

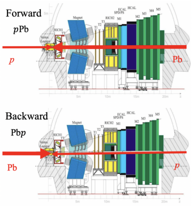

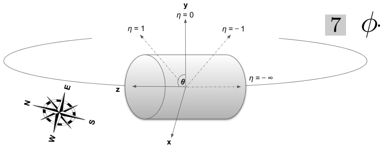

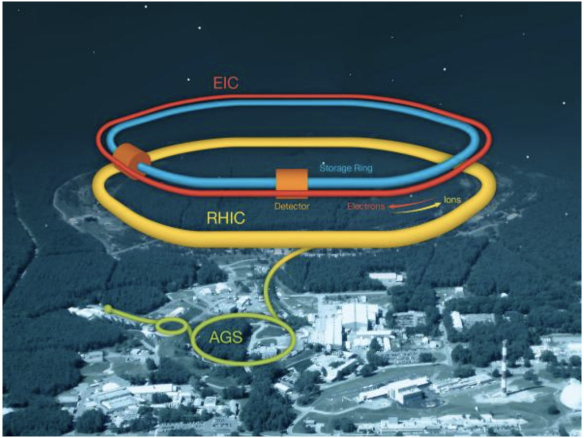

Small System Results

Charged Hadron Modification in p+Al

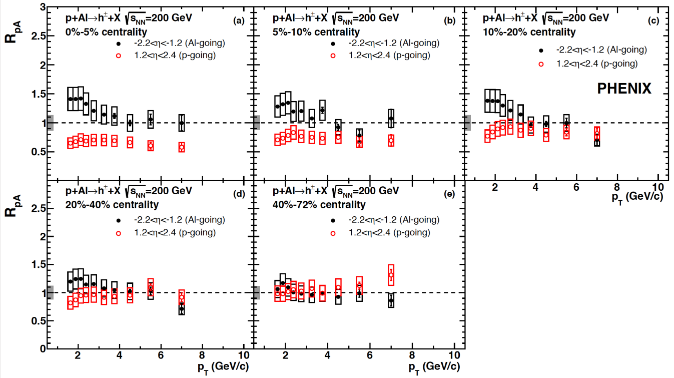

- Minimal modification in most peripheral bin$^{40-72\%}$
- Clear suppression in most central bin$^{0-5\%}$ in projectile-going direction (fwd)
- Clear enhancement in 0-5% bin in target-going direction (bkwd)
  - $\langle N_{part}^{0-5\%} \rangle = 5.1$

Phys. Rev. C 101, 034910 (2020)

Charged Hadron Modification in p+Au

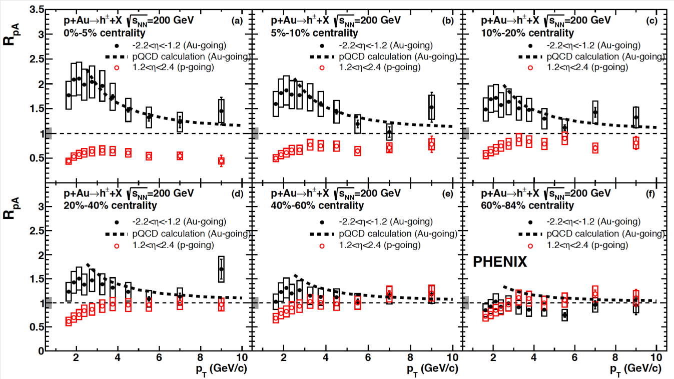

- Minimal modification in most peripheral bin$^{60-84\%}$
- Strongest suppression in most central bin$^{0-5\%}$
  - $\langle N_{part}^{0-5\%} \rangle = 10.7$
- Strong enhancement in most central bin$^{0-5\%}$ in target-going direction (bkwd)
  - Consistent with pQCD calculation

Phys. Lett. B 740,23

Phys. Rev. C 101, 034910 (2020)

Charged Hadron Modification in p+Al and p+Au

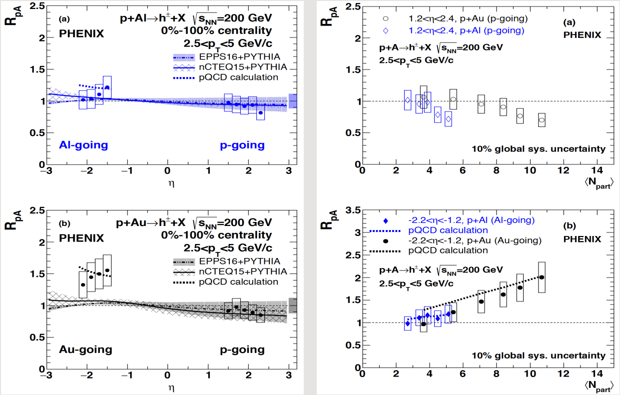

- All models at fwd rapidity agree well with R_{pA} as function of η
- Models for R_{pAu} at backward rapidity as function of η:
  - nCTEQ15 and EPPS15 models underpredict enhancement
  - pQCD model describes data well **Phys. Lett. B 740,23**
- pQCD calculations for RpA bkwd rapidity as function of $\langle N_{part}\rangle$ also agree with data

Phys. Rev. C 101, 034910 (2020)

ϕ Modification in Small Systems

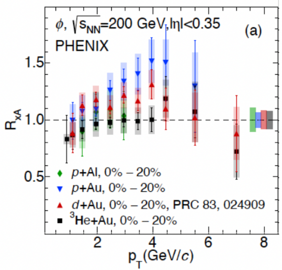

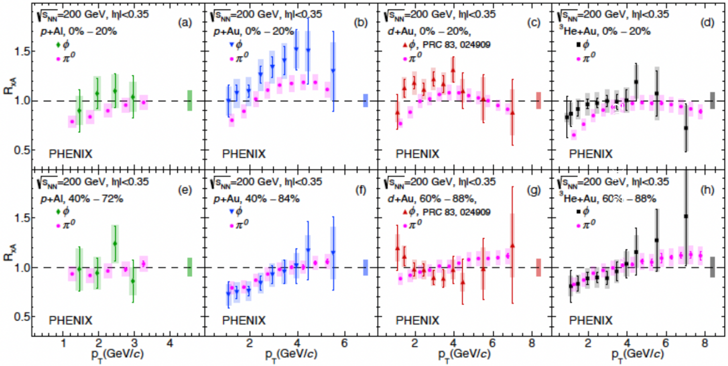

PRC 106 (2022) 1, 014908

- ϕ-meson nuclear modification in p+Al, p+Au, d+Au, and ^{3}He+Au systems
  - Hint of experimental ordering of $R_{HeAu} < R_{dAu} < R_{pAu}$ in most central collisions (?)
- Comparison of ϕ $(s, \bar{s})$ to π^0 (u, d) shows no clear strangeness enhancement

$b\bar{b}$ Invariant Yields in $p+p$ Collisions

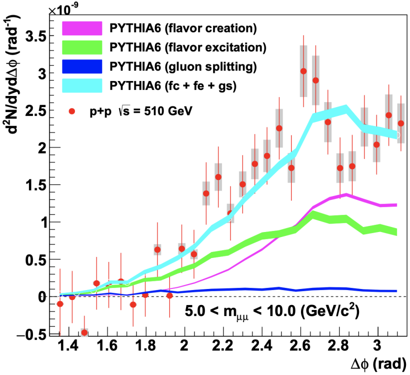

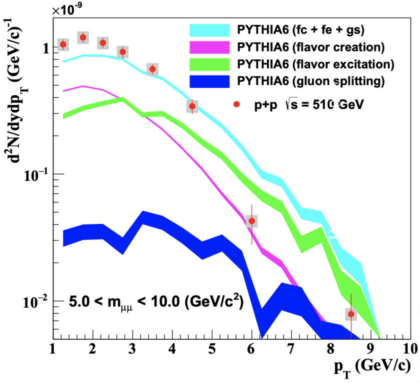

PHYS. REV. D 102, 092002 (2020)

- Comparison of PYTHIA6 models based on different $b\bar{b}$ production mechanisms
  - Flavor creation and flavor excitation mechanisms dominate production
    - At RHIC energies, gluon splitting less significant than at LHC energies

$\sigma_{b\bar{b}}$ vs. $\sqrt{s}$ in $p+p$ Collisions

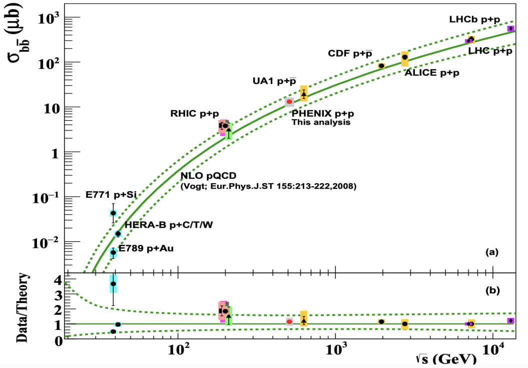

Phys. Rev. D 102, 092002 (2020)

- Bottom cross section $\sigma_{b\bar{b}}$ as a function of $\sqrt{s}$ for PHENIX, STAR, HERA-B, ALICE, LHCb
  - Cross section measurement consistent with world data
  - Data well described by NLO pQCD calculation [1]

Angular Coefficients

Pedagogical illustration of the decay angular distribution

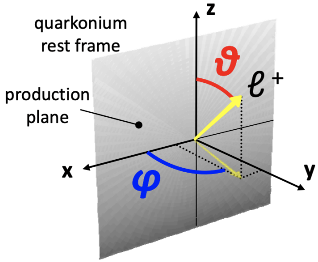

$$W(\cos\theta,\varphi) \propto 1 + \lambda_\theta \cos^2\theta + \lambda_{\theta\varphi} \sin 2\theta \cos\varphi + \lambda_\varphi \sin^2\theta \cos 2\varphi$$

$$\tilde{\lambda} = \frac{\lambda_\theta + 3\lambda_\phi}{1 - \lambda_\phi}$$

P. Faciolli, Quarkonium in Hot Medium (2009) and Eur. Phys. J. C 69, 657 (2010)

- J/ψ polarization characterized by spin alignment of positively charged decay lepton
- $\lambda_\theta, \lambda_\phi$ and $\lambda_{\theta\phi}$ determined using Helicity, Collins–Soper, or Gottfried–Jackson frames
- $\lambda_\theta = \{+1, 0, -1\} \Rightarrow$ fully transverse, fully zero, or fully longitudinal J/ψ polarization
- Frame invariant angular decay coefficient $\tilde{\lambda}$ can be used for consistency check

J/ψ Polarization λ_θ

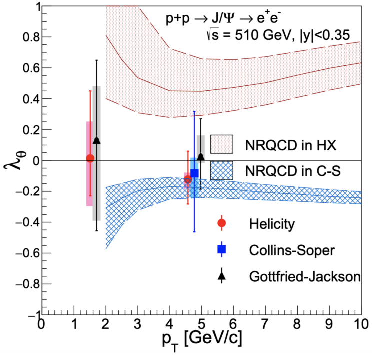

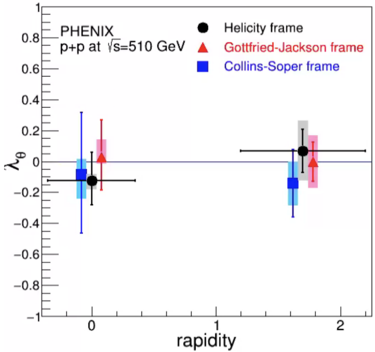

Phys. Rev. D 102, 072008 (2020)

- J/ψ polarization as a function of p_T in all three frames is consistent with zero
  - NRQCD Model [2] in both Helicity and Collins–Soper frames agrees with data
- J/ψ polarization at both mid and forward rapidity consistent with zero

J/ψ Polarization $\tilde{\lambda}$

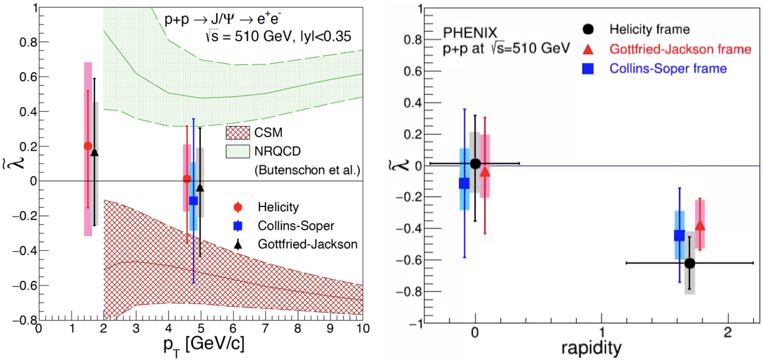

Phys. Rev. D 102, 072008 (2020)

- J/ψ polarization as a function of p_T in all three frames is consistent with zero
  - Neither NRQCD or Color Singlet Models [3] can be ruled out
- At forward rapidity, J/ψ polarization consistent with longitudinal polarization

J/ψ Production, Forward Rapidity

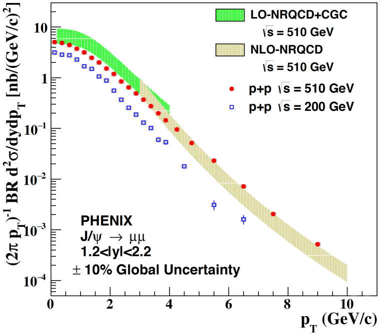

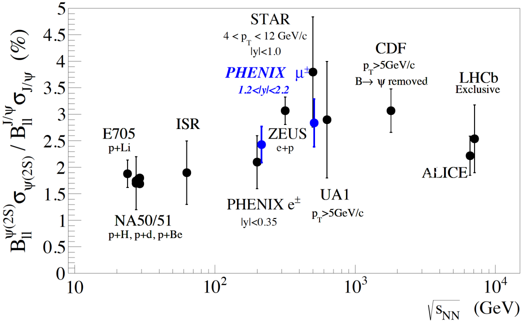

Phys. Rev. D 101, 052006 (2020)

- Inclusive J/ψ differential cross section compared to prompt J/ψ calculations
  - Non-prompt J/ψ contribution more significant at high p_T
  - LO NRQCD+Color Glass Condensate [4] at low p_T overestimates data
- $\psi(2S)/J/\psi$ ratio consistent with world data - no clear energy dependence

J/ψ Production in pp Collisions

Prompt

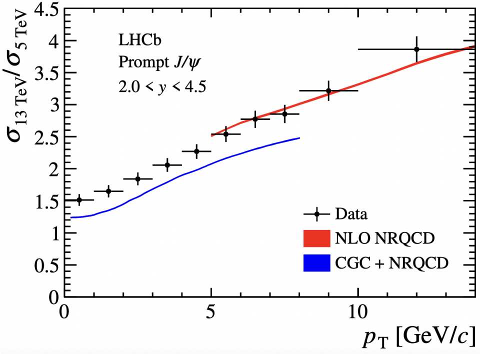

Nonprompt

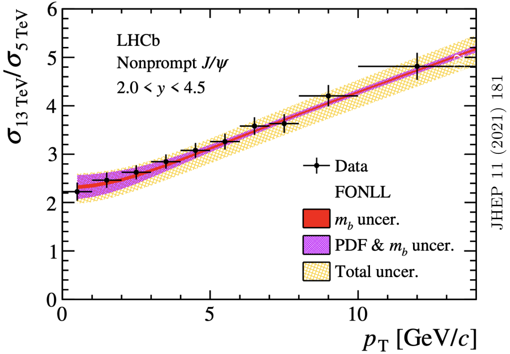

- Ratio of differential J/ψ cross-section at 13 TeV vs. 5 TeV increases with p_T
  - Discrepancy between prompt J/ψ ratio & CGC+NRQCD [4] (errors mostly cancel)
  - Nonprompt J/ψ data consistent with FONLL [5] predictions as function of p_T

J/ψ Nuclear Modification in pPb Collisions

$$R_{pPb} = \frac{\sigma_{pPb}}{208 \times \sigma_{pp}}$$

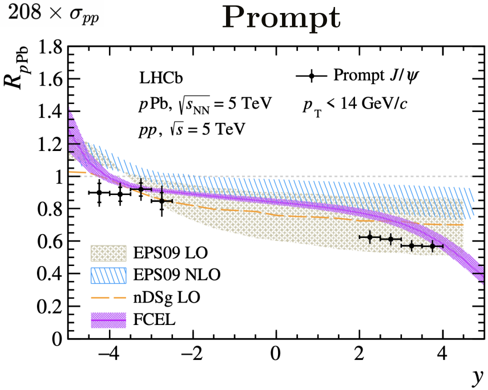

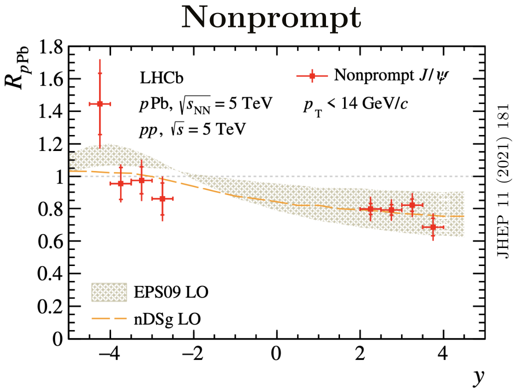

- At forward rapidity, prompt and nonprompt J/ψ nuclear modification consistent with nPDF predictions (EPS09 LO, nDSg LO) [6]
- Prompt J/ψ R_{pPb} more suppressed than EPS09 LO, NLO for $-4.5 < y < -2$

EPS Shadowing Predictions, 2008

Low-x gluon nuclear densities

- Current knowledge of low-x gluons from: F_2 (e-A), Drell-Yan (p-A), high-p_T hadrons (d-Au).
- x<0.01: very few measurements (non-perturbative): huge uncertainties !

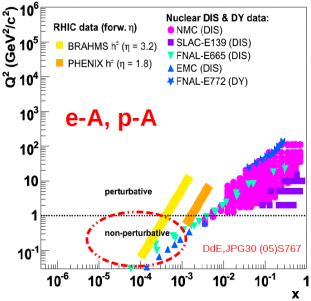

K.Eskola et al. JHEP 0807 (08)102

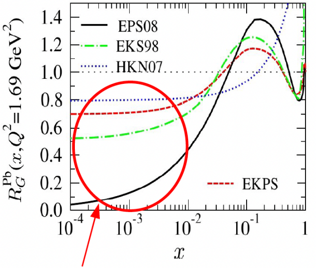

$xG(x,Q^2)$ virtually unknown below $x \sim 10^{-2}$!

Slide credit: David d'Enterria (2011)

LHC D-meson Measurements

$$Q^2_{exp} = m^2 + p_T^2 \qquad x_{exp} = \frac{Q_{exp}}{\sqrt{S_{NN}}} e^{-y_{CM}}$$

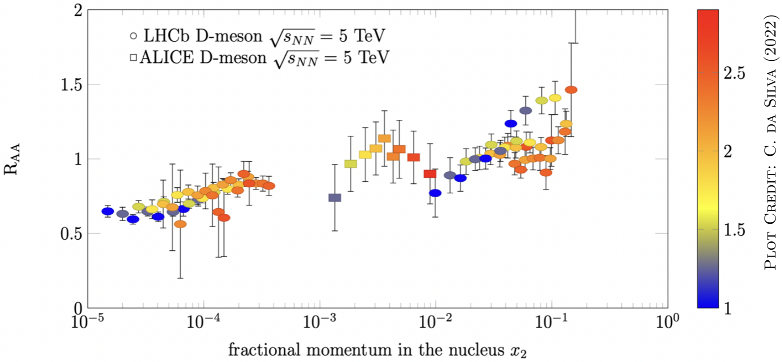

- LHCb and ALICE D-meson nuclear modification plotted as a function of Bjorken-x
  - Data extended now beyond x^{-4} fractional momentum in the nucleus

J/ψ Nuclear Modification in p+Au Collisions

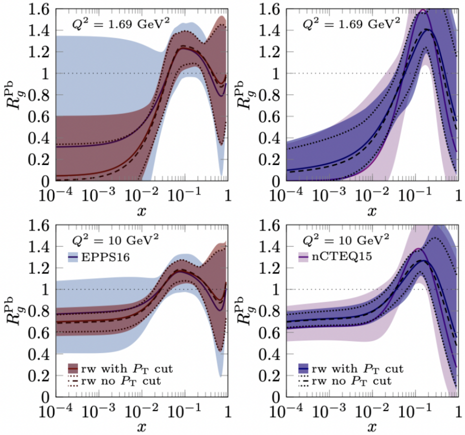

JHEP 05 (2020) 037

⋆ See Tony Frawley's talk, Week 2

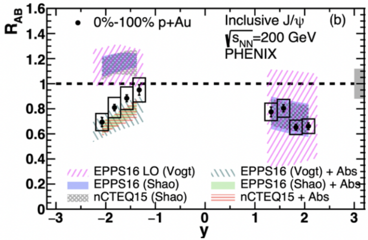

Phys. Rev. C 102, 014902

- EPPS16 and nCTEQ15 with and without re-weighted LHCb D-meson data
  - Re-weighted EPPS16 and nCTEQ15 describe PHENIX data well at forward rapidity ⋆

Bottomonium Nuclear Modification in pPb Collisions

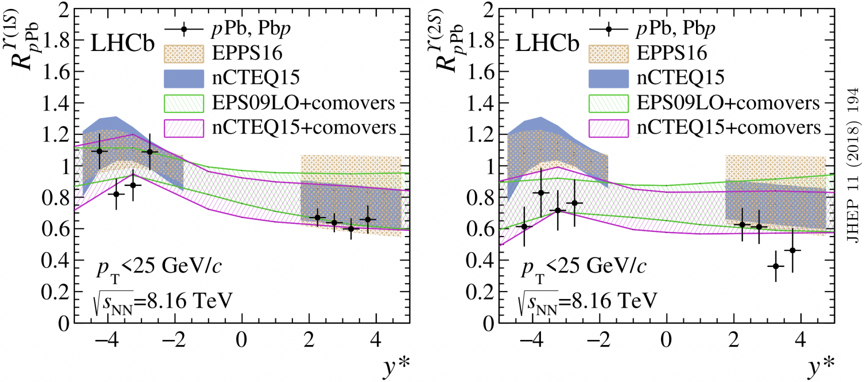

- At both forward and backward rapidity, hint of stronger $\Upsilon(2S)$ suppression than $\Upsilon(1S)$
- At backward rapidity, nPDFs alone do not fully describe modification of either state
  - nPDF+comovers [7] calculations provide better description of data

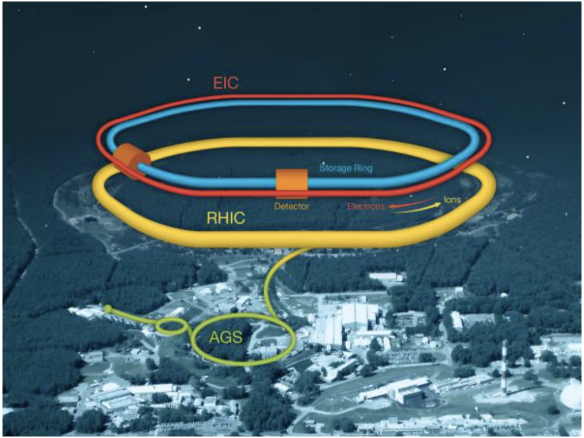

Medium to Large System Results

J/ψ & D^0 Production in PbNe Collisions

Fixed Target

$$\frac{\sigma_{J/\psi}}{\sigma_{D^0}} = \frac{\sigma^{pp}_{J/\psi}}{\sigma^{pp}_{D^0}} \times \langle N_{coll}^{\alpha'-1} \rangle = C' \times \langle N_{coll}^{\alpha'-1} \rangle$$

Phys. Letters B 410 (1997) 337-343 [NA50]

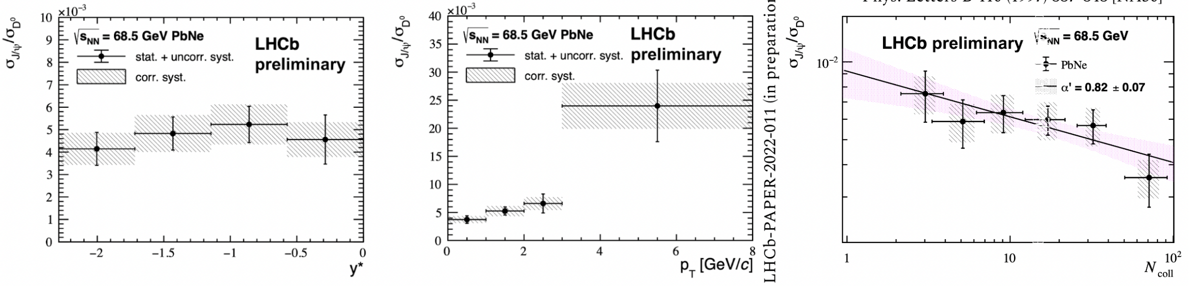

- Fixed target configuration with p or Pb projectiles at GeV COM energies
  - Noble gases injected into VELO using SMOG (System for Measuring Overlap with Gas)
- Fit to ratio of J/ψ to D^0 vs. N_{coll} consistent with NA50 results in p+A collisions
  - α' indicates no anomalous J/ψ suppression as seen in NA50 PbPb results

J/ψ Elliptic Flow in Au+Au Collisions

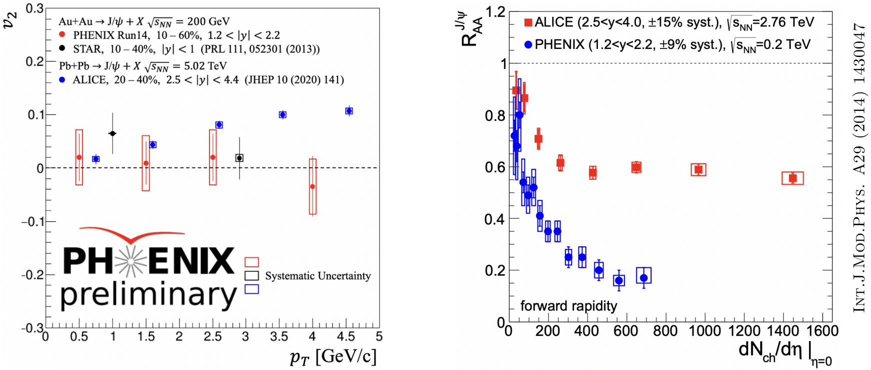

- J/ψ elliptic flow in Au+Au at RHIC compared with LHC PbPb measurements
- Nonzero elliptic flow at LHC could be due to coalescence, which is stronger effect at LHC energies than at RHIC energies

Coherent J/ψ Production in PbPb UPC

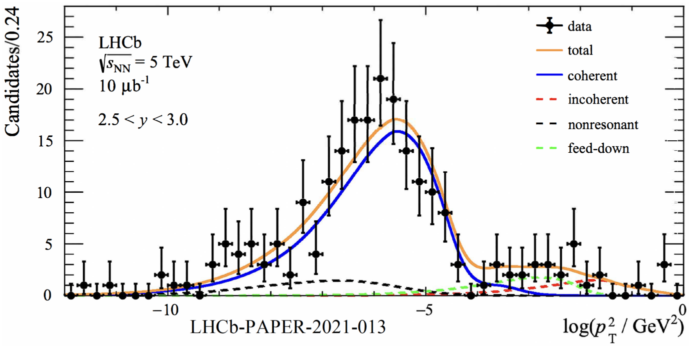

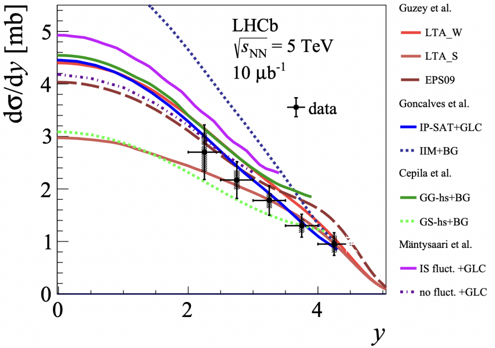

- Fit to the log of p_T^2 distribution performed to isolate coherent from incoherent production
- Differential cross-section for coherent J/ψ production decreases as function of y
  - Several of the CGC-based predictions (blue dotted, solid magenta & solid green curves) overestimate the J/ψ production

Coherent $\psi(2S)$ Production in PbPb UPC

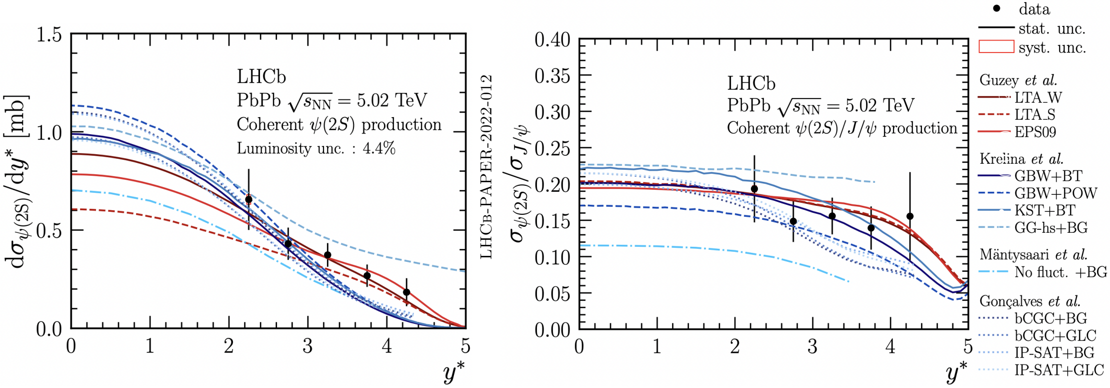

- First measurement at LHC for coherent $\psi(2S)$ production at forward rapidity
    - pQCD calculations (red curves) by Guzey *et al.* describe data well at large y
- Ratio of $\psi(2S)$ to J/ψ not as well described by CGC predictions (blue curves)

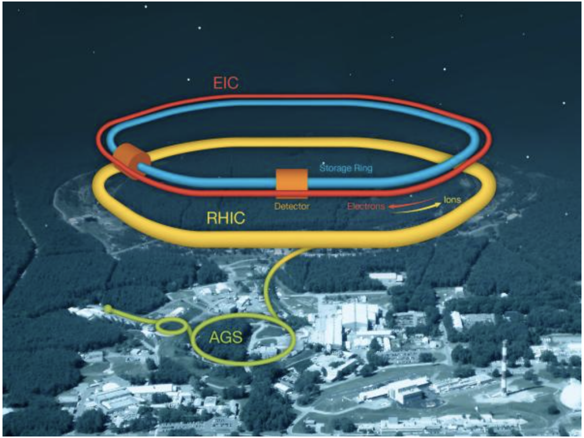

Summary

Quarkonia and Heavy Flavor Summary

① J/ψ Production in pp and pPb Collisions
- Discrepancy between prompt J/ψ data and CGC+NRQCD at low p_T
- Prompt J/ψ R_{pPb} more suppressed than EPS09 NLO for $-4.5 < y < -2$

② Bottomonium Nuclear Modification in pPb Collisions
- Hint of stronger $\Upsilon(2S)$ than $\Upsilon(1S)$ suppression at both rapidities
- At backward rapidity, nPDFs alone do not fully describe modification

③ J/ψ and D^0 Production in Fixed Target PbNe Collisions
- Ratio of J/ψ to D^0 vs. N_{coll} shows no anomalous QGP suppression

④ Charmonium Production in Ultra-Peripheral PbPb Collisions
- First measurement of coherent ψ(2S) production at forward rapidity
- Ratio of coherent ψ(2S) to J/ψ consistent with pQCD predictions

④ Elliptic Flow in Haevy-Ion Collisions
- J/ψ elliptic flow in A+A collisions consistent with zero at RHIC energies

Theoretical References

[1] Vogt, R.
The total charm cross section
Eur.Phys.J.ST 155 (2008) 213-222

[2] Butenschoen, M. and Kniehl, B.
J/ψ Polarization at the Tevatron and the LHC: Nonrelativistic-QCD Factorization at the Crossroads,
Phys.Rev.Lett. 108 (2012) 17200

[3] Butenschoen, M. and Kniehl, B.
Next-to-leading order tests of nonrelativistic-QCD factorization with J/ψ yield and polarization
Mod.Phys.Lett.A 28 (2013) 1350027

[4] Ma, Yan-Qin and Wang, Kai and Chao, Kuang-Ta
J/ψ(ψ') production at the Tevatron and LHC at $\mathcal{O}(\alpha_s^4 v^4)$ in nonrelativistic QCD
Phys. Rev. Lett. 106 (2011) 042002

[5] Cacciari, M. and Mangana, Michelangelo and Nason, Paolo
Gluon PDF constraints from the ratio of forward heavy-quark production at the LHC at $\sqrt{s} = 7$ and 13 TeV
Eur. Phys. J. C75 (2015) 610

[6] Ferreiro, E.G. and Fleuret, F. and Lansberg, J.P.
Impact of the Nuclear Modification of the Gluon Densities on J/ψ production in pPb collisions at $\sqrt{s_{NN}} = 5$ TeV
Phys. Rev. C 88 (2013) 4, 047901

[7] Ferreiro, Elena and Lansberg, Jean-Philippe
Is bottomonium suppression in proton-nucleus and nucleus-nucleus collisions at LHC energies due to the same effects?
J. High Energy Phys. 10 (2018) 094

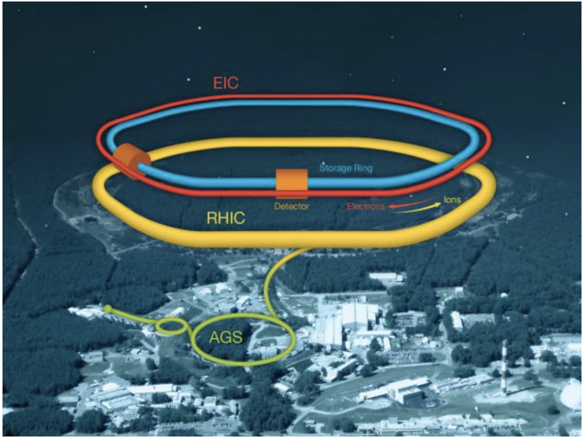

Back-Up

ϕ Elliptic Flow in Cu+Au Collisions

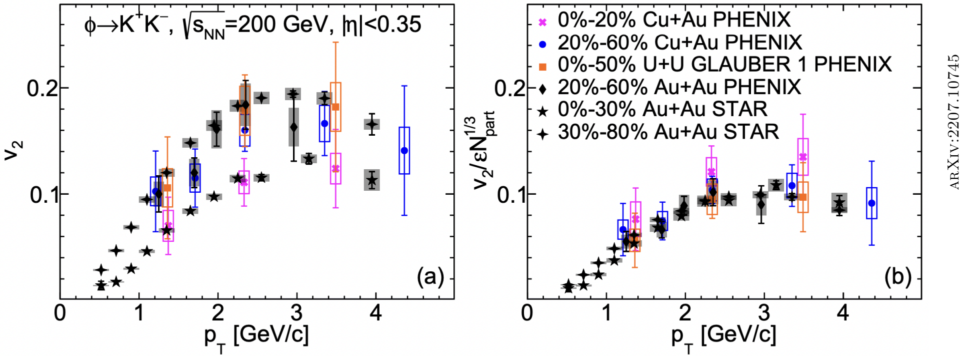

- Elliptic flow of ϕ-meson shown in symmetric (Au+Au, U+U) versus anti-symmetric (Cu+Au) collision systems
  - Scaling with participant eccentricity of second order (ϵ_2) represents dependence of v_2 on shape of nuclear overlap region

More Information on ϕ Elliptic Flow

collisions by PHENIX [38] and in 0%–30% and 30%–80% Au+Au collisions by STAR [52] are also shown in Fig. 8. The comparison of elliptic flow for ϕ mesons in symmetric and asymmetric collision systems suggests that the v_2 values follow common empirical scaling with $\varepsilon_2 N_{\rm part}^{1/3}$. Scaling with participant eccentricity of second order ε_2 represents dependence of v_2 on the shape of the nuclear overlap region. The $N_{\rm part}^{1/3}$ factor is introduced to characterize the length scale of nuclear overlap region and assumed to be proportional to the QGP length scale [19]. This suggests that the influence of the initial conditions on v_2 coefficients, and thereby on QGP properties, are reasonably well encapsulated in the scaling factor $\varepsilon_2 N_{\rm part}^{1/3}$. The scaling of v_2 values with the shape and size of nuclear-overlap region can be explained by the hydrodynamic nature of the QGP at low values of specific-shear viscosity [21].

arXiv 2207.10745

LHCb heavy ion collision modes and datasets

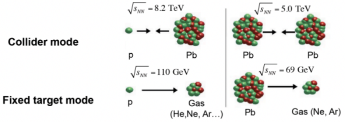

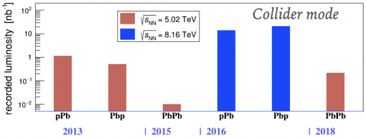

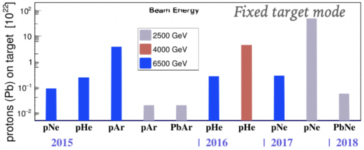

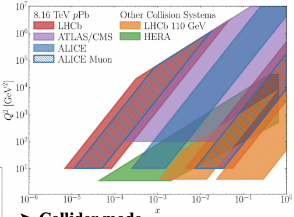

➤ **Collider mode**

- pPb/Pbp:
  - 5.02 TeV and 8.16TeV
  - Probes saturation region and small Bjorken-x physics
- PbPb: centrality-limited to 60%

➤ **Fixed-target mode (SMOG)**

- pNe, pHe, pAr: $\sqrt{s_{NN}} \sim 100$ GeV
- PbNe: $\sqrt{s_{NN}} \sim 68.6$ GeV
- Covers mid to backward rapidity: anti-shadowing region

➤ ***p*Pb/Pb*p* rapidity coverage**

- y^*: rapidity in nucleon-nucleon cms
- $y^* = y \pm 0.465$
- Forward: $1.5 < y^* < 4.0$
- Backward: $-5.0 < y^* < -2.5$
- Common region: $2.5 < |y^*| < 4.0$

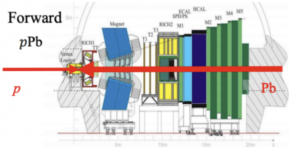

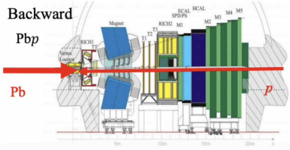

Credit: Jiayin Sun, Quark Matter 2022

Quarkonium in pp collisions

- Charmonium (J/ψ, $\psi(2S)$) in pp collisions:
  - Prompt: originate from the primary pp collision vertex
  - Nonprompt: originate from b-decay vertex
- Bottomonium (Υ) in pp collisions: only prompt
- To separate prompt and nonprompt charmonium
  - Pseudo decay time

$$\text{forward}-y\text{: } t_z = \frac{z_\psi - z_{\text{PV}}}{p_z/m_\psi} \qquad \text{mid}-y\text{: } \tau = \frac{L_{xy}}{p_{\text{T}}/m_\psi}$$

Vertex Locator at LHCb

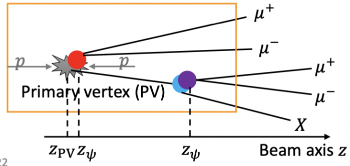

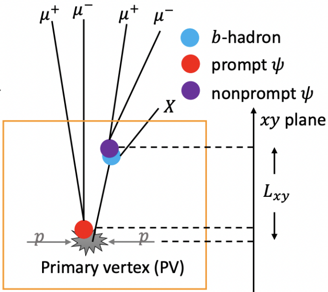

Inner Detector at ATLAS

Jan 10, 2022 6

Credit: Li Xu, Quarkonium as Tools 2022

A large Scintillating Fibre Tracker for LHCb

Daniel Berninghoff, Physikalisches Institut, Heidelberg University
on behalf of the LHCb Scintillating Fibre Tracker Collaboration

The LHCb Detector

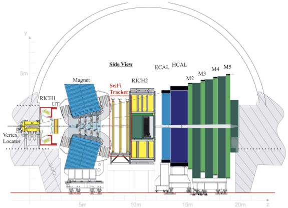

The upgraded LHCb detector.

Single-arm forward spectrometer with a pseudorapidity acceptance between 2 and 5 that is specialised in the search of new physics in beauty and charm hadron decays

LHCb Upgrade: 2019-2022

Upgrade of the LHCb detector to increase the precision on key observables and extend its physics reach by obtaining 5 to 10 times higher signal yields.

- ⇒ 5 times higher instantaneous luminosity
- ⇒ Triggerless 40 MHz readout
- ⇒ New front- and back-end electronics
- ⇒ **Replacement of complete tracking system**

The Scintillating Fibre (SciFi) Tracker

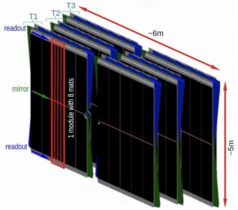

Large and high granular scintillating fibre tracker that is readout by arrays of silicon photomultipliers (SiPMs).

- 3 stations (T1, T2, T3) with 4 layers each
- Covering a total area of 340 m^2
- 1 % X_0 per layer
- Spatial resolution < 100 µm
- Single hit efficiency ~99 %
- 524 288 channels in total
- 250 µm fibre diameter and channel width
- 40 MHz readout
- ~20 Tb/s data rate

Credit: Daniel Berninghoff, CERN-Poster-2021-1047

Nuclear effects & asymmetric acceptance

"forward"
Measured particles at $\eta > 0$
Probes low x in nuclear PDF

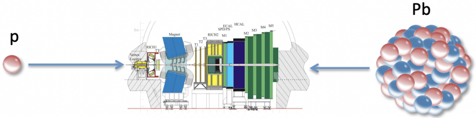

“backward”
Measured particles at $\eta < 0$
Probes high x in nuclear PDF

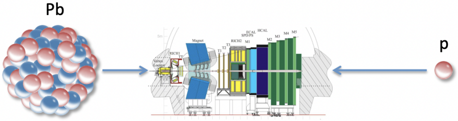

Nuclear modification factor

$$R_{pPb} = \frac{\text{cross-section for pPb}}{A_{Pb} \text{ x cross-section for pp}}$$

No nuclear effects: $R_{pPb} = 1$

Forward-Backward (FB) ratio

$$R_{FB} = \frac{\text{cross-section for pPb } +|y|}{\text{cross-section for pPb } -|y|}$$

Credit: Hans Dembinski, Deep Inelastic Scattering 2019

SMOG: fixed-target program

SMOG: System for Measuring Overlap with Gas.

Noble gases at a pressure of O(10^{-7}) mbar are injected into the VELO.

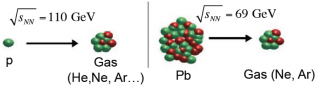

$$y = y^* + ln(\frac{\sqrt{s_{NN}}}{m_p})$$

$$x_F \simeq \frac{2}{\sqrt{s_{NN}}}\sqrt{M^2 + p_T^2} \quad sinh(y^*)$$

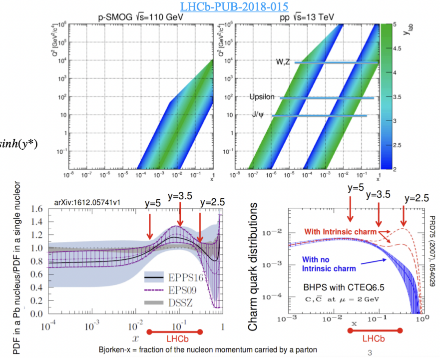

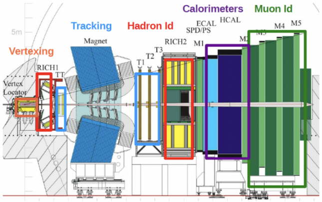

JINST 3 (2008)S08005

- $-3.0 < y^* < 0$
- Probe intrinsic charm content in the nucleon.
- Access nPDF anti-shadowing region.

Credit: Sara Sellam, Strangeness in Quark Matter 2022

Centrality determination in PbNe

16

- The centrality of a nucleus-nucleus → overlap region between the nuclei where the nucleons are colliding.
- MC Glauber model used to to isolate the hadronic part and subsequently define the centrality classes
- Proxy: energy deposit in the ECAL (VELO clusters saturates)

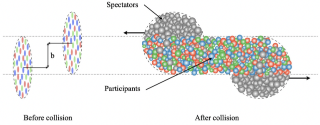

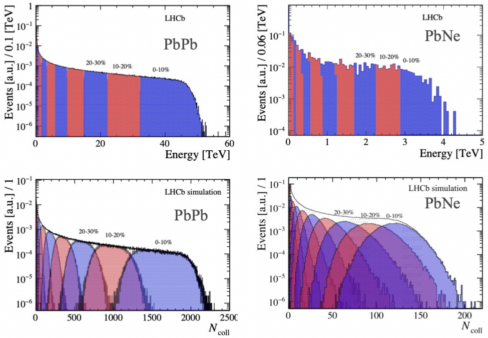

CERN-LHCb-DP-2021-002
https://arxiv.org/pdf/2111.01607.pdf

Credit: Elisabeth Maria Niel, Large Hadron Collider Physics 2022